

# Comparison of infrared canopy temperature in a rubber plantation and tropical rain forest

Qing-Hai Song<sup>1,2</sup> · Yun Deng<sup>1,3,4</sup> · Yi -Ping Zhang<sup>1,2</sup> · Xiao-Bao Deng<sup>1,3</sup> ·  
You-Xing Lin<sup>1,2,4</sup> · Li-Guo Zhou<sup>1,2,4</sup> · Xue-Hai Fei<sup>1,2,4</sup> · Li-Qing Sha<sup>1,2</sup> ·  
Yun-Tong Liu<sup>1,2</sup> · Wen-Jun Zhou<sup>1,2</sup> · Jin-Bo Gao<sup>1,2,4</sup>

Received: 3 April 2016 / Revised: 5 May 2017 / Accepted: 5 May 2017 / Published online: 31 July 2017  
© ISB 2017

**Abstract** Canopy temperature is a result of the canopy energy balance and is driven by climate conditions, plant architecture, and plant-controlled transpiration. Here, we evaluated canopy temperature in a rubber plantation (RP) and tropical rainforest (TR) in Xishuangbanna, southwestern China. An infrared temperature sensor was installed at each site to measure canopy temperature. In the dry season, the maximum differences ( $T_c - T_a$ ) between canopy temperature ( $T_c$ ) and air temperature ( $T_a$ ) in the RP and TR were 2.6 and 0.1 K, respectively. In the rainy season, the maximum ( $T_c - T_a$ ) values in the RP and TR were 1.0 and −1.1 K, respectively. There were consistent differences between the two forests, with the RP having higher ( $T_c - T_a$ ) than the TR throughout the entire year. Infrared measurements of  $T_c$  can be used to calculate canopy stomatal conductance in both forests. The difference in ( $T_c - T_a$ ) at three  $g_c$  levels with increasing direct radiation in the RP was larger than in the TR, indicating that

change in ( $T_c - T_a$ ) in the RP was relatively sensitive to the degree of stomatal closure.

**Keywords** Surface temperature · Tropical · Rainforest · Rubber plantation · Climate change

## Introduction

Infrared canopy temperature ( $T_c$ ) measurements can be conducted rapidly and efficiently, and are an alternative to conventional methods, such as stomatal conductance ( $g_c$ ) or stem water potential measurements, for monitoring plant water status in different agricultural and forest ecosystems (Leuzinger and Köner 2007; Wang and Gartung 2010; Maes et al. 2011; Scherrer et al. 2011; Ballester et al. 2013). For example, when crops are managed under deficit irrigation, infrared thermometry can provide useful information regarding surface temperature for supporting variable-rate irrigation in time and space and identification of irrigation zones (Alchanatis et al. 2010; Cohen et al. 2011). Canopy foliage temperature is a comprehensive result of plant traits, energy balance, and environmental factors (Scherrer et al. 2011). Therefore, different plant species or communities are highly variable in  $T_c$  due to biotic and abiotic variables, which might have different cooling effects.

Plants under soil water deficit often decrease  $g_c$ , resulting in reduced transpiration and increased leaf temperature. Therefore,  $g_c$  plays an important role in plant–atmosphere water exchange. Instruments such as infrared gas analyzers or porometers have been used to determine the stomatal opening (Zhang et al. 2007; Chen 2008; Zhang et al. 2013, 2014) by measuring the transpiration rate on a small portion of leaves. However, these measurements are labor intensive and non-automated, which limits the spatial and temporal coverage of  $g_c$  assessments. In addition, using

**Electronic supplementary material** The online version of this article (doi:10.1007/s00484-017-1375-4) contains supplementary material, which is available to authorized users.

✉ Qing-Hai Song  
sqh@xtbg.ac.cn

✉ Yi -Ping Zhang  
yipingzh@xtbg.ac.cn

<sup>1</sup> Key Laboratory of Tropical Forest Ecology, Xishuangbanna Tropical Botanical Garden, Chinese Academy of Sciences, Menglun 666303, China

<sup>2</sup> Global Change Ecology Group, Xishuangbanna Tropical Botanical Garden, Chinese Academy of Sciences, Menglun 666303, China

<sup>3</sup> Xishuangbanna Station for Tropical Rain Forest Ecosystem Studies, Chinese Ecosystem Research Net, Mengla, Yunnan 666303, China

<sup>4</sup> University of Chinese Academy of Sciences, Beijing 100049, China

these methods, it is difficult for technicians to sample the canopy leaves of dominant tree species and measure the leaf  $g_c$  in tropical forests with old trees and a high canopy (Leuzinger and Köner 2007; Scherrer et al. 2011). Fortunately, previous studies have shown that with a few supplemental measurements and application of biophysical principles, infrared measurement of  $T_c$  can be used to calculate canopy  $g_c$  (Leinonen et al. 2006; Blonquist et al. 2009; Leuzinger et al. 2010).

Xishuangbanna, located at the northern edge of tropical southwestern Asia, is a transitional area between the tropics and the subtropics. The area is considered to be particularly sensitive to the impacts of climate change (Tan et al. 2013; Zhang et al. 2015), such as changes in temperature and precipitation patterns. Climate records at Xishuangbanna over the past 40 years have shown a significant increase in air temperature ( $T_a$ ). A previous study showed that the expansion of rubber plantations and the reduction of tropical seasonal rainforest would likely induce local surface warming and larger ranges in daily temperature (Lin et al. 2009). Monoculture rubber plantations and primary tropical forests are highly variable in physiological traits related to the water balance. Therefore, the change in  $T_c$  in relation to the responses of the two communities to expected climate change might also be variable.

The objectives of this study were to (1) to quantify the differences in magnitude and seasonal dynamics of  $T_c$  in the two forest ecosystems, (2) evaluate the usefulness of thermography for the estimation of canopy  $g_c$ , and (3) discuss differences in  $T_c$  between the two forest ecosystems in a changing climate.

## Site and methods

### Site describe

The tropical rainforest study site (TR) (21° 55' 39" N, 101° 15' 55" E, 750 m a.s.l.) is located in the Menglun Nature Reserve in Xishuangbanna, southwestern China (Fig. 1).

The site is located at the northern edge of tropical southwestern Asia, and is a transition area between the tropics and the subtropics (Zhang 1966; Cao et al. 1996). The dry season occurs between November and April. Dominant tree species are *Pometia tomentosa*, *Terminalia myriocarpa*, *Gironniera subaequalis*, and *Garuga floribunda*, which can exceed 40 m in height (Fig. 2). The soil is lateritic derived from siliceous rocks, such as granite and gneiss, with a pH from 4.5 to 5.5.

The rubber plantation study site (RP) is located in the experimental area of the Xishuangbanna Tropical Botanical Garden (21° 55' 30" N, 101° 15' 59" E; elevation 570 m a.s.l.), Xishuangbanna, Yunnan Province, southwestern China (Fig. 1). Rubber plantations (*Hevea brasiliensis*) have been replacing primary TR with dramatic speed in recent years in China (Song et al. 2013). The study site is included in a large 36-year-old rubber plantation. The rubber plantation has a mean canopy height of approximately 22 m (Fig. 2).

The two sites are located about 10 km apart and share similar climate conditions. According to climatic observations at a meteorological station over the past half century (1959–2008), the mean annual temperature is 21.8 °C, and the mean annual rainfall is 1511 mm. Over 85% of the annual rainfall occurs in the rainy season. The mean monthly rainfall during the dry season is less than 40 mm.

**Fig. 1** Location of the study site (XSBN: Xishuangbanna)

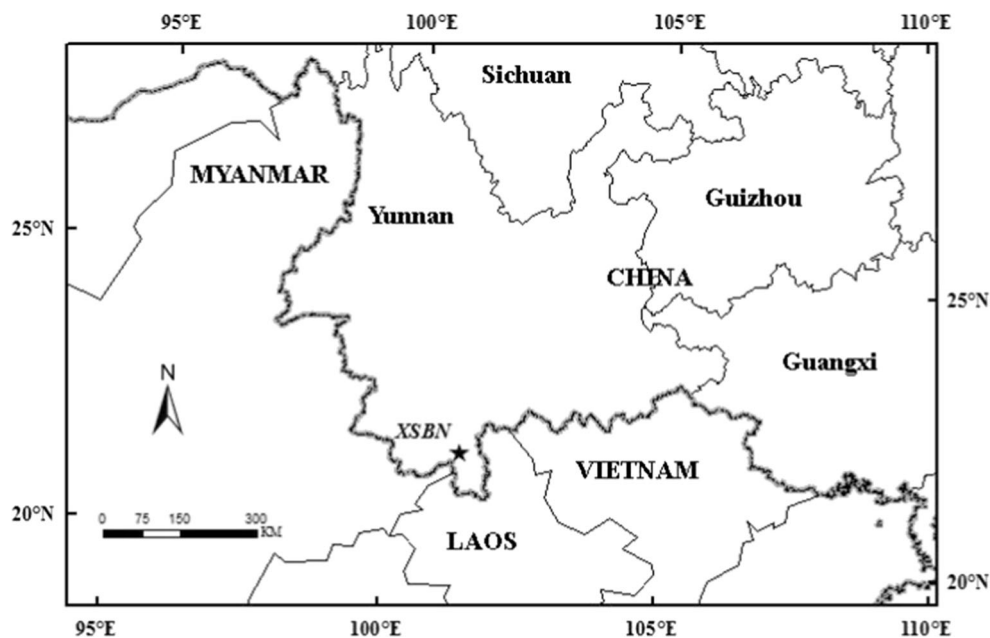
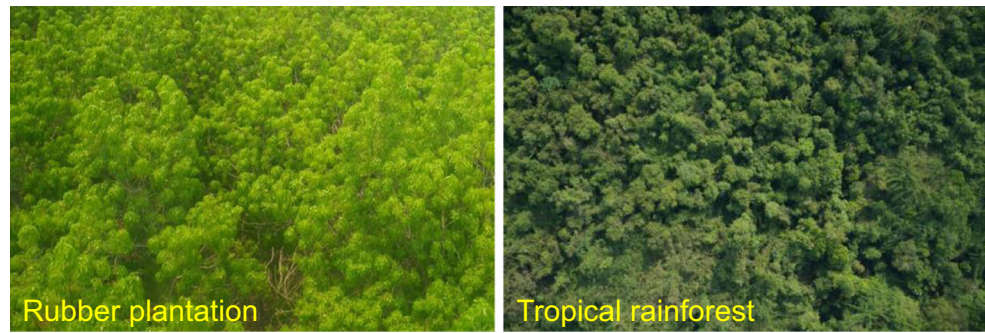


**Fig. 2** Canopy pictures of the rubber plantation and the tropical rainforest



### Measurement of meteorological factors and $T_c$

Instruments for measuring  $T_a$ , air humidity (RH) (HMP45C, Vaisala, Helsinki, Finland), and wind speed ( $W_s$ ) (A100R, Vector Instruments, Denbighshire, UK) were installed on the observational tower at each site. Radiation sensors for downward and upward, short- and long-wave radiation (CNR-1/CM11, Kipp & Zonen, Delft, Netherlands) were installed on a horizontal pole 3 m from the tower at each site. Profiles of soil moisture were measured at different depths (5, 10, 20, 40, 60, and 100 cm) (105 T/107 L, Campbell, Logan, UT, USA) at each site. Meteorological data were collected every 30 min at each site using a CR1000 (Campbell).

An infrared temperature sensor (SI-111, Apogee Instruments, Inc., Logan, UT, USA) was installed at each site to measure  $T_c$ . The sensor was installed on an observational tower and mounted on 4-cm-diameter galvanized metal pipes positioned 3.0 m above each forest canopy. The sensor was aimed at the canopy, with view half angles of approximately  $22^\circ$  from nadir. The absolute accuracy of the sensor is  $\pm 0.2^\circ\text{C}$ . The radiation detected using an infrared radiometer includes two components: (1) the radiation directly emitted by the target surface, and (2) reflected background radiation. The second component is often neglected. The magnitude of the two components in the radiation detected by the radiometer is estimated using the emissivity and reflectivity of the target surface (Blonquist et al. 2009).

### Leaf area index measurement

Leaf area index (LAI) was measured using a canopy analyzer (Model LAI-2000, LI-COR, Lincoln, NE, USA). We measured the background value (termed A value by LAI-2000) at the top of the tower in the TR (70 m) and the RP (55 m). The LAI at different heights was measured at platform locations on the towers. On each platform, 15 points were sampled in different directions to eliminate the tower shadow effect. The LAI was measured monthly in the two sites.

### Calculating canopy stomatal conductance

$H_c$  is sensible heat flux and  $\lambda E_c$  is latent heat flux. The terms  $H_c$  and  $\lambda E_c$  can be expressed as (Campbell and Norman 1998)

$$H_c = g_H C_p (T_c - T_a) \quad (1)$$

$$\lambda E_c = g_T \lambda \left( \frac{\text{VPD}}{P_a} \right) \quad (2)$$

where  $g_H$  is the boundary layer heat conductance ( $\text{mmol m}^{-2} \text{s}^{-1}$ ),  $C_p$  is the specific heat of air at constant pressure ( $\text{J mol}^{-1} \text{K}^{-1}$ ),  $g_T$  is the total water vapor conductance ( $\text{mmol m}^{-2} \text{s}^{-1}$ ),  $\lambda$  is the latent heat of vaporization ( $\text{J mol}^{-1}$ ), VPD is the vapor pressure deficit (kPa), and  $P_a$  is the atmospheric pressure (kPa)

$$g_T = \frac{1}{\left( 1/g_H \right) + \left( 1/g_c \right)} \quad (3)$$

Combining Eqs. (1)–(3) and rearranging to solve for canopy  $g_c$  ( $\text{mmol m}^{-2} \text{s}^{-1}$ ) (Blonquist et al. 2009) yields

$$g_c = \frac{g_H P_a [(R_n - G) - g_H C_p (T_c - T_a)]}{g_H \lambda \text{VPD} - P_a [(R_n - G) - g_H C_p \text{VPD}]} \quad (4)$$

where  $P_a$  is the atmospheric pressure (kPa),  $R_n$  is the net radiation ( $\text{W m}^{-2}$ ), and  $G$  is the soil heat flux ( $\text{W m}^{-2}$ ).

Based on the terms of the Monin–Obukhov similarity theory (Monin and Obukhov 1954),  $g_H$  is discerned between conductance of heat and the boundary layer conductance of water vapor.

### Analysis method

A multiple correlation regression analysis (SPSS 22.0 Software, SPSS Inc. 2013, IBM, Armonk, NY, USA) was used for the stepwise selection of the dominant drivers of  $g_c$  during the dry season, rainy season, and whole year. The drivers for  $g_c$ , as included in this analysis, were solar radiation (DR),  $T_a$ , vapor pressure deficit (VPD), and  $W_s$ . The dominant

variables for each regression were chosen by a stepwise procedure. The coefficients and their relative contributions are presented for each variable.

## Results

### $T_c$ variability

Figure 3 shows  $T_a$ ,  $T_c$ , and the diurnal canopy to air temperature difference ( $T_c - T_a$ ) during the dry season (March–April) and rainy season (July–August) in 2011 at the two sites.

In general, the variation patterns of  $T_a$  in the same season at the two sites were similar (Fig. 3). However,  $T_c$  was different at the two sites in the same season. The value of canopy to air temperature difference ( $T_c - T_a$ ) at the RP was higher than the TR throughout the entire study period. During the dry season, the daily peak value of ( $T_c - T_a$ ) at RP appeared to occur at approximately 12:00 h (Fig. 3a), while the daily peak value of ( $T_c - T_a$ ) at TR appeared to occur at 13:00 h (Fig. 3b). The maximum ( $T_c - T_a$ ) values at the RP and TR in the dry season were 2.6 and 0.1 K (Fig. 3a, b), respectively. During the rainy season, the daily peak value of ( $T_c - T_a$ ) at the RP appeared to

occur at approximately 13:00 h, while the peak value at the TR appeared around 15:30 h. During nighttime, ( $T_c - T_a$ ) at the TR was significantly lower than the RP. The maximum ( $T_c - T_a$ ) values at the RP and TR in the rainy season were 1.0 and −1.1 K, respectively.

### Infrared temperature for estimating canopy stomatal conductance

Continuous estimation of canopy  $g_c$  based on the infrared temperature at both study sites is shown in Fig. 4.  $g_c$  showed clear seasonal patterns in RP.  $g_c$  was nearly zero during the leafless period at the end of the foggy-cool season (Fig. 4), and then  $g_c$  increased sharply with leaf emergence in the early dry-hot season.  $g_c$  reached a high plateau during the rainy season. The value of  $g_c$  peaked after the leaf flush, and the maximum  $g_c$  was about  $750 \text{ mmol m}^{-2} \text{ s}^{-1}$  in the rainy season.  $g_c$  became lower with leaf senescence and then declined rapidly during leaf fall (Fig. S1).

In general,  $g_c$  also showed a seasonal pattern in TR. However,  $g_c$  showed a higher day-to-day variation than in the RP during the rainy season.

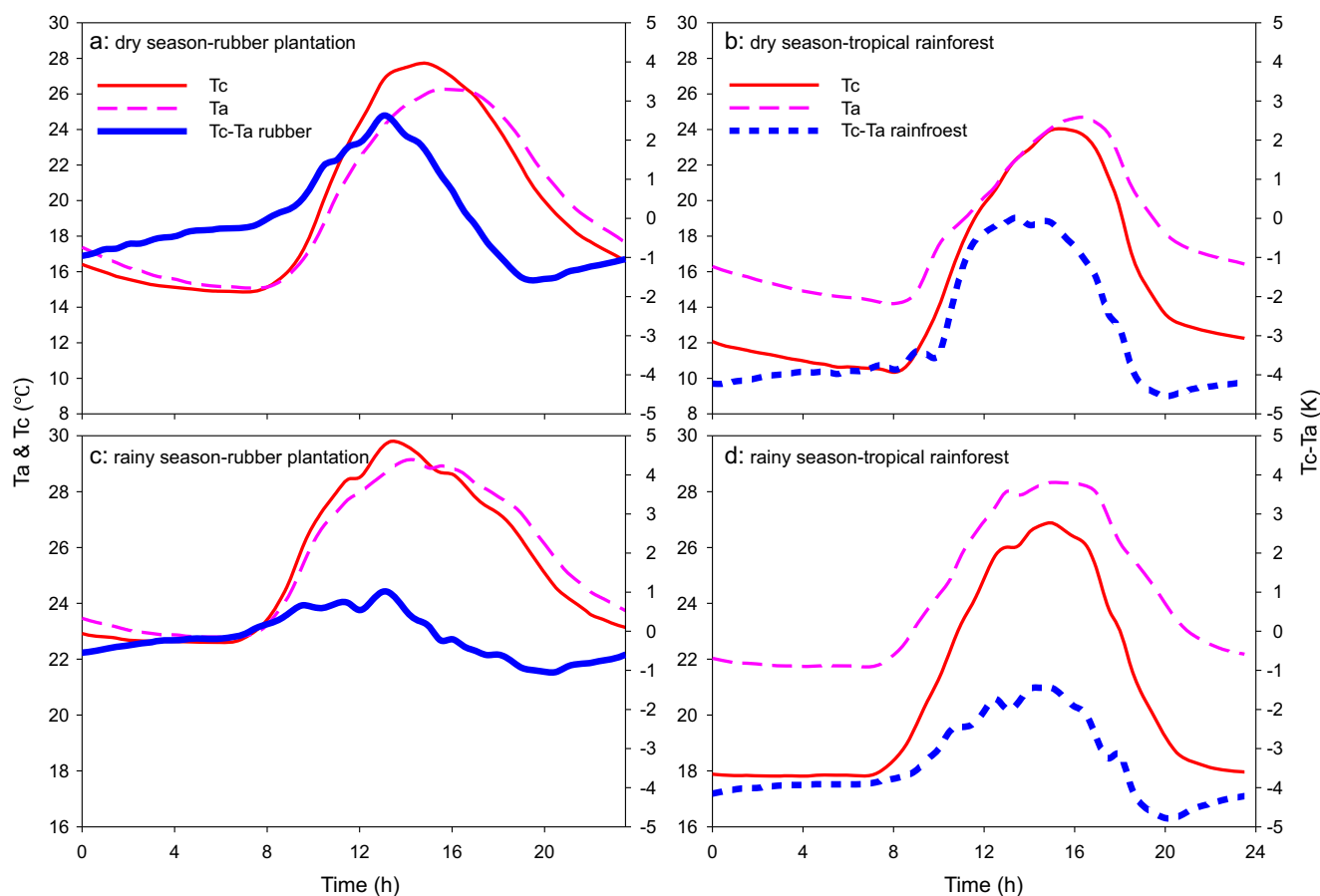


**Fig. 3** Mean diurnal time series of air to canopy temperature difference during dry and rainy seasons in 2011 at the rubber plantation and tropical rainforest sites (**a** dry season rubber plantation; **b** dry season tropical rainforest; **c** rainy season rubber plantation; **d** rainy season tropical rainforest)



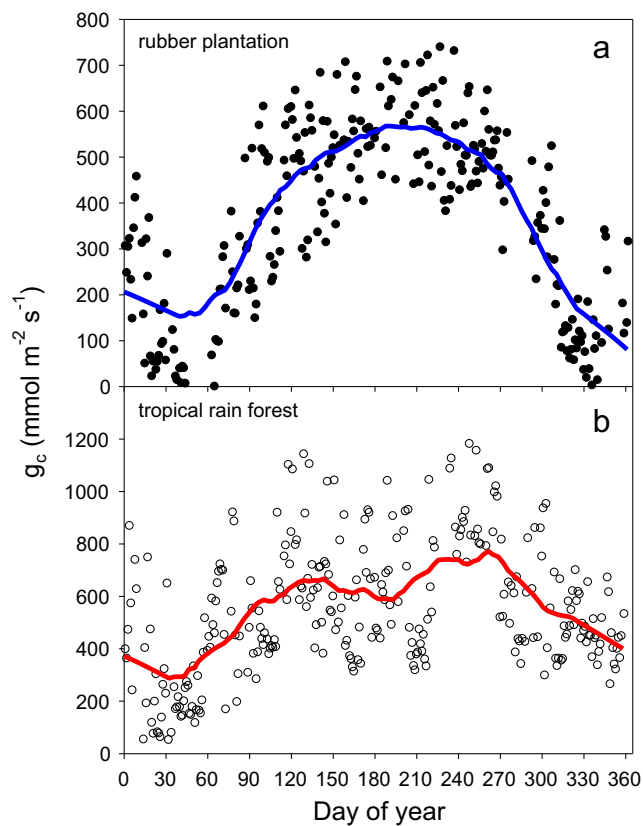


**Fig. 4** Continuous estimation of canopy stomatal conductance ( $g_c$ ) based on infrared temperature in the rubber plantation (**a**) and tropical rain forest (**b**). The values are average of six half-hour averages from 12:00 to 15:00 h. The *blue* and *red lines* represent daily average over daytime

We derived the energy balance for a plant canopy to calculate canopy stomatal conductance from measured meteorological and plant variables, which provided field-scale measurements of daily and seasonal stomatal response to local climate conditions.

To more deeply explore the influence of microclimate factors on  $g_c$  under the varying climatic conditions, we evaluated the correlations of environmental conditions with  $g_c$  on a statistical basis during the dry season and rainy season and over the entire year in RP and TR.

Multivariable correlations between  $g_c$  and microclimate conditions are shown in Table 1. The analysis defines the relative contribution of each parameter to  $g_c$ .  $T_a$  is the primary factor correlated with  $g_c$  during the dry season in the two sites. The relative contributions of each parameter to  $g_c$  were similar in the two forests. During the rainy season, VPD was the most important variable ( $\beta\% = 57\%$ ) in the TR, but  $T_a$  was still the most influential ( $\beta\% = 40\%$ ) in the RP. The relative contribution of  $T_a$  and RH were almost equivalent in the two forests. The two climate variables,  $T_a$  and VPD, contributed a total of 80% of the variations to  $g_c$  in the two forests over the entire year.

### $T_c - T_a$ variations in a changing climate

To discuss possible effects of a changing climate on canopy-to-air temperature differences in the future, we solved Eq. 5 to evaluate the variations of  $T_c$ :

$$T_c - T_a = \frac{Pa(Rn - G) - g_c \lambda VPD + (g_c / gH) Pa(Rn - G)}{g_c C_p + gH C_p VPD} \quad (5)$$

Increasing drought frequency has the potential to affect the carbon and water cycle in forest ecosystems. Warmer global temperatures are expected to cause an intensification of the hydrologic cycle, with increased evaporative demand in ecosystems. As mentioned above, plants under drought stress decrease stomatal conductance, thereby reducing transpiration and increasing  $T_c$ . Therefore, to explore the differences in  $T_c$  between RP and TR in an expected changing climate, we assumed a decrease by 25, 50, and 75% of maximum  $g_c$  values at both sites.

In order to better evaluate the difference of  $T_c$  in the two forests,  $(T_c - T_a)$  was normalized by  $T_a$  ( $[T_c - T_a]_{\text{normalized}}$ ).  $(T_c - T_a)_{\text{normalized}}$  was very sensitive to all simulated meteorological conditions (Fig. 5) and increased linearly with increasing DR.  $(T_c - T_a)_{\text{normalized}}$  decreased non-linearly with

**Table 1** Coefficients (B) and relative contributions ( $\beta\%$ ) of meteorological parameters with  $g_c$  of the rubber plantation (RP) and tropical rainforest (TR) in different periods

	Dry season				Rainy season				Whole year			
	RP		TR		RP		TR		RP		TR	
	B	$\beta\%$	B	$\beta\%$	B	$\beta\%$	B	$\beta\%$	B	$\beta\%$	B	$\beta\%$
DR	-0.1	18*	-0.3	5	-1.0	20**	0.1	10*	-0.9	12**	-0.7	13*
$T_a$	50.0	51**	31.4	51**	54.9	40**	4.2	24**	57.0	60**	23.6	52**
VPD	-268.9	29**	-267.0	39**	-315.8	33**	-22.4	57**	-328.0	24**	-70.6	28**
$W_s$	32.3	2	-189.9	5	60.4	7	79.2	9*	53.9	4	-267.0	7

\*Significant difference for the parameter between the different periods at the 0.05 significance level; \*\*difference at the 0.01 significance level

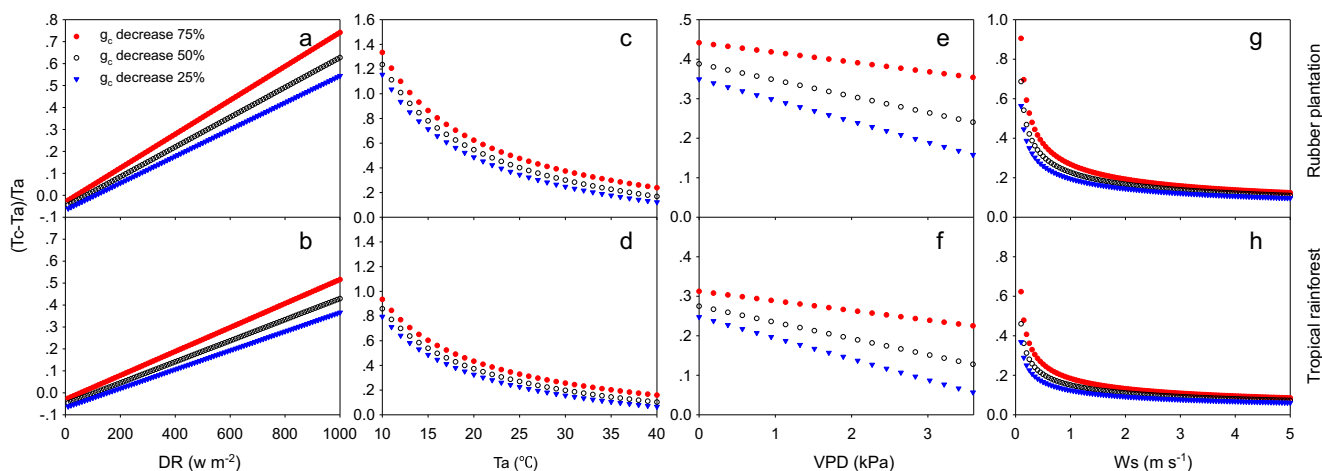


**Fig. 5** Influence of climate conditions on  $(T_c - T_a)_{\text{normalized}}$ , including direct radiation (DR), air temperature ( $T_a$ ), vapor pressure

deficit (VPD), and wind speed ( $W_s$ ), for three levels of  $g_c$  at the rubber plantation (a, c, e, g) and the tropical rainforest sites (b, d, f, h)

increasing  $T_a$  and  $W_s$  (Fig. 5).  $(T_c - T_a)_{\text{normalized}}$  increased sharply with DR in all  $g_c$  levels and at all sites. At the same level of  $g_c$ ,  $(T_c - T_a)_{\text{normalized}}$  had a steeper increase in relation to increasing DR in RP than in TR (Fig. 5a, b) on average, approximately 2 K higher than in TR. However, the difference in  $(T_c - T_a)_{\text{normalized}}$  at three  $g_c$  levels with increasing DR in RP was larger than in TR, indicating that change in the  $(T_c - T_a)_{\text{normalized}}$  in RP was relatively sensitive to the degree of stomatal closure. In contrast, the difference in  $(T_c - T_a)_{\text{normalized}}$  at the three  $g_c$  levels in TR became smaller with increasing DR.

$(T_c - T_a)_{\text{normalized}}$  showed a completely opposite pattern than that of increasing  $T_a$  and VPD (Fig. 5c–f), indicating that  $(T_c - T_a)_{\text{normalized}}$  decreased with increasing VPD. Similarly, the difference of  $(T_c - T_a)_{\text{normalized}}$  at three  $g_c$  levels with increasing  $T_a$  in TR was small, while the difference was large in RP. In TR,  $(T_c - T_a)_{\text{normalized}}$  decreased slightly with increasing  $T_a$ , indicating that  $(T_c - T_a)_{\text{normalized}}$  did not particularly depend on  $T_a$  at low  $g_c$  levels. In contrast,  $(T_c - T_a)_{\text{normalized}}$  was highly sensitive to increasing  $T_a$  in TR due to a relatively more opened stoma and higher canopy transpiration.

## Discussion

Our results showed constant difference between the two forests, with the RP having a higher  $(T_c - T_a)$  than the TR throughout the whole year. The greater heating of canopy leaves in RP is likely the result of general low canopy  $g_c$ , leading to low transpirative cooling. Plants under soil water deficit decrease  $g_c$ , thereby reducing transpiration and increasing leaf temperature. Previous study has shown that canopy transpiration for dominant tree species in the dry season was lower than in the rainy season at both sites (Song et al. 2013). The reduction in transpiration in the dominant canopy trees

during the dry season (with high evaporative demand) could partly explain the increase of canopy to  $T_a$  difference. Our results were consistent with thermodynamic principles that posit that a more “developed” ecosystem should have relatively lower surface temperature than a less developed equivalent (Schneider and Kay 1994; Lin et al. 2009).

Canopy  $g_c$  has been used as a parameter to express the physical effect of stomatal movement at the canopy scale (Maruyama and Kuwagata 2008; Zhang et al. 2011). Infrared  $T_c$  measurements provided a useful evaluation of canopy conductance in monoculture plantation and primary TR in this study. The maximum  $g_c$  in the RP was higher than the value ( $500 \text{ mm m}^{-2} \text{ s}^{-1}$ ) in a teak plantation in Northern Thailand (Igarashi et al. 2015). The maximum  $g_c$  in TR was similar with the  $g_c$  ( $1200 \text{ mm m}^{-2} \text{ s}^{-1}$ ) in a tropical forest in Nigeria (Grace et al. 1982). With the estimated LAI, we transferred  $g_c$  ( $\text{mmol m}^{-2} \text{ s}^{-1}$ ) to stand-level conductance ( $\text{mm s}^{-1}$ ,  $g_s$ ). The maximum  $g_s$  in TR was about  $2.70 \text{ mm s}^{-1}$ , which was higher than the average  $g_s$  ( $2.2 \text{ mm s}^{-1}$ ) in a tropical forest in Brazil (Pereira et al. 2010) and similar with the average  $g_s$  ( $2.67 \text{ mm s}^{-1}$ ) in an olive orchard in southern Spain (Testi et al. 2006).

In addition, infrared  $T_c$  measurements are automatic and effective, providing an alternative option to conventional methods, such as stomatal conductance or stem water potential measurements, in monitoring plant water status (Wang and Gartung 2010; Ballester et al. 2013), especially in the tropical forests with a high canopy. For example, the LAI of RP during the rainy season was about  $3.9\text{--}4.6 \text{ m}^2 \text{ m}^{-2}$ . Daily  $g_c$  mean values during the rainy season (per projected leaf area) ( $500\text{--}750 \text{ mmol m}^{-2} \text{ s}^{-1}$ ) in RP were typically about three to five times that of the single leaf values (per projected leaf area,  $100\text{--}180 \text{ mmol m}^{-2} \text{ s}^{-1}$ ) (Chen 2008). This is consistent with the finding that canopies with multiple leaf layers have higher conductance than single leaves due to the sum of contributions from the single leaves (Blonquist et al. 2009). Our results also

support the big-leaf model theory, which maps properties of the whole canopy onto a single leaf (Zhang et al. 2011). However, monitoring  $T_c$  with the infrared temperature sensor in a fixed position only partially covers the canopy, and the data are too limited to account for variations in the entire canopy and differences between species, particularly for the high diversity tropical forest in this study. Previous study has also shown that canopy architecture has a consistent influence on canopy foliage temperature, in that “dense canopy” species are warmer than “open canopy” species in a mixed temperate forest (Scherrer et al. 2011). In contrast, we can see that the canopy is not always continuous in the forest and some canopy gaps are embedded in the community. Monitoring  $T_c$  with the infrared temperature sensor might include information from big branches and the forest floor. In addition, the temperature of shaded leaves is lower than the sunlit leaves of the same trees (Ballester et al. 2013).

As mentioned previously, the TR canopy is uneven and complex and can be divided into three layers. The fixed infrared sensor cannot measure the lower layer temperature, resulting in an underestimation of the actual leaf temperature of fully sun-exposed leaves, and therefore, it presented mean canopy foliage temperature in TR. Furthermore, the higher day-to-day variation in TR suggested that this fact could be due to the difficulty of relating the average temperature of multiple differently oriented leaves with stomatal conductance of individual ones. In this study, the canopy of RP was more flat and homogenous, and the use of  $T_c$  measurements to detect canopy  $g_c$  appeared to be more precise in RP than in TR. It appeared that  $g_c$  in TR showed higher day-to-day variation than in RP during the rainy season, indicating that the high tree species diversity in TR influenced the final canopy  $g_c$  pattern.  $g_c$  may strongly depend on canopy architecture (leaf area density, branching habits, and canopy height) in combination with leaf traits. For the tall forest, it has been shown that transfer coefficients of different layers may differ quite significantly during the daytime (Raupach 1979; Viswanadham and Sa 1987). Below the canopy, the flow is likely to be influenced by thermal effects directly attributable to the surface (Raupach 1979). Therefore, the different layers of tall forests should be considered in future studies.

Despite the fact that the two sites shared similar climate conditions, stand structure and topography also impacted the difference between  $T_c$  and  $T_a$ . On a daily scale,  $T_c$  increased rapidly as soon as the sun struck the canopy. The canopy of the TR, which was located in a valley, warmed slowly in the morning and cooled rapidly in the evening.

In addition, characterizing infrared sensor noise is imperative for ensuring that thermal fluctuations are attributable to the forest canopy (Aubrecht et al. 2016). Estimation of canopy stomatal conductance can be improved by dividing the canopy into sunlit and shaded leaves (Wang and Leuning 1998; Irmak et al. 2008). Also, there was no correction for evaporation of

intercepted water and fog/cloud drip and the effect of canopy cooling during the rainy season or part of the dry season. Intercepted water, fog drip, and cloud shading regulate the forest water balance, VPD, and vegetation  $g_c$ . Suppressed incoming radiation and transpiration rates during the fog period of the dry season may be favorable for low water use in these study sites. Future work is needed to improve estimates of the variation in canopy conductance on a fine spatial scale and diurnal and seasonal time scales (Aubrecht et al. 2016).

Normalized  $(T_c - T_a)$  was very sensitive to all simulated meteorological conditions. Normalized  $(T_c - T_a)$  increased linearly with increasing DR and decreasing VPD. Normalized  $(T_c - T_a)$  also decreased non-linearly with increasing  $T_a$  and  $W_s$ . Our simulation results were consistent with research by Maes et al. (2011), Maes and Steppe 2012). Overall,  $T_c$  in the RP and TR responded differently to the changing climate. The change in  $T_c$  was controlled by the climate, but plant-inherent traits, such as  $g_c$ , also played an important controlling role. Despite the fact that infrared  $T_c$  measurements can be used as a water stress indicator, there has yet to be a critical assessment of the relationship between  $T_c$  and plant species composition, canopy structure, and leaf functional traits.

**Acknowledgements** We thank Jun-Bin Zhao, Jun-Fu Zhao, Lei Yu, and Meng-Nan Liu for their assistance in the field. This study was funded by the National Natural Science Foundation of China (41671209, U1602234), the Yunnan Natural Science Foundation of Yunnan Province, China (2013FB077), and the National Key Research and Development Program of China (2016YFC0502105). We gratefully appreciate detailed comments of the anonymous reviewers on an earlier version of this manuscript.

#### Compliance with ethical standards

**Competing interests** The authors declare that there are no competing interests.

## References

- Alchanatis V, Cohen Y, Cohen S, Moller M, Sprinstin M, Meron M, Tsipris J, Saranga Y, Sela E (2010) Evaluation of different approaches for estimating and mapping crop water status in cotton with thermal imaging. *Precis Agric* 11:27–41
- Aubrecht DM, Helliker BR, Goulden ML, Roberts D., Still CJ, Richardson AD (2016) Continuous, long-term, high-frequency thermal imaging of vegetation: uncertainties and recommended best practices. *Agric For Meteorol* 315–326
- Ballester C, Jiménez-Bello MA, Castel JR, Intrigliolo DS (2013) Usefulness of thermography for plant water stress detection in citrus and persimmon trees. *Agric For Meteorol* 168:120–129
- Blonquist JM Jr, Norman JM, Bugbee B (2009) Automated measurement of canopy stomatal conductance based on infrared temperature. *Agric For Meteorol* 149:2183–2197
- Campbell GS, Norman JM (1998) An introduction to environmental biophysics. Springer, New York

- Cao M, Zhang J, Feng Z, Deng J, Deng X (1996) Tree species composition of a seasonal rain forest in Xishuangbanna, southwestern China. *Trop Ecol* 37:183–192
- Chen JW (2008) Water relations, photosynthetic performance and physiological protection in *Hevea brasiliensis* in the marginal tropical area, Xishuangbanna, SW China. Graduate School of Chinese Academy of Sciences for the degree of Ph.D. P13
- Cohen Y, Alchanatis V, Prigojin A, Levi A, Soroker V, Cohen Y (2011) Use of aerial thermal imaging to estimate water status of palm trees. *Precis Agric*
- Grace J, Okali DUU, Fasehun FE (1982) Stomatal conductance of two tropical trees during the wet season in Nigeria. *J Appl Ecol* 19(2):659
- Igarashi Y, Kumagai T, Yoshifuji N, Sato T, Tanaka N, Tanaka K, Suzuki M, Tantasirin C (2015) Environmental control of canopy stomatal conductance in a tropical deciduous forest in northern Thailand. *Agric For Meteorol* 202(15):1–10
- Irmak S, Mutiibwa D, Irmak A, Arkebauer TJ, Weiss A, Martin DL, Eisenhauer DE (2008) On the scaling up leaf stomatal resistance to canopy resistance using photosynthetic photon flux density. *Agric For Meteorol* 148:1034–1044
- Leinonen I, Grant OM, Tagliavia C, Chaves MM, Jones HG (2006) Estimating stomatal conductance with thermal imagery. *Plant Cell Environ* 29(8):1508–1518
- Leuzinger S, Köner C (2007) Tree species diversity affects canopy leaf temperatures in a mature temperate forest. *Agric For Meteorol* 146:29–37
- Leuzinger S, Vogt R, Köner C (2010) Tree surface temperature in an urban environment. *Agric For Meteorol* 150(1):56–62
- Lin H, Cao M, Stoy PC, Zhang YP (2009) Assessing self-organization of plant communities—a thermodynamic approach. *Ecol Model* 220:784–790
- Maes WH, Steppe K (2012) Estimating evapotranspiration and drought stress with ground-based thermal remote sensing in agriculture: a review. *J Exp Bot* 63:4671–4712
- Maes WH, Achten WMJ, Reubens B, Muys B (2011) Monitoring stomatal conductance of *Jatropha curcas* seedlings under different levels of water shortage with infrared thermography. *Agric For Meteorol* 151:554–564
- Maruyama A, Kuwagata T (2008) Diurnal and seasonal variation in bulk stomatal conductance of the rice canopy and its dependence on developmental stage. *Agric For Meteorol* 148:1161–1173
- Monin AS, Obukhov AM (1954) Basic laws of turbulent mixing in the ground layer of the atmosphere. Tr. Geofiz. Inst. Akad. Nauk, SSSR no. 24 (151). In: Goering H (ed) *Sammelband zur Statistischen Theorie der Turulenz* (German translation 1958). Akademie Verlag, Berlin, pp 163–187
- Pereira DD, De Mello CR, Silva AM, Yanagi S (2010) Evapotranspiration and estimation of aerodynamic and stomatal conductance in a fragment of Atlantic Forest in mantiqueira range region, MG. *Cerne* 16(1):32–40
- Raupach MR (1979) Anomalies in flux-gradient relationships over forest. *Bound-Layer Meteorol* 16:467–486
- Scherrer D, Bader MKF, Köner C (2011) Drought-sensitivity ranking of deciduous tree species based on thermal imaging of forest canopies. *Agric For Meteorol* 151:1632–1640
- Schneider ED, Kay JJ (1994) Life as a manifestation of the second law of thermodynamics. *Math Comput Model*:25–48
- Song QH, Lin H, Zhang YP, Tan ZH, Zhao JF, Zhao JB, Zhang X, Zhou WJ, Yu L, Yang LY, Yu GG, Sun XM (2013) The effect of drought stress on self-organisation in a seasonal tropical rainforest. *Ecol Model* 265:136–139
- Tan ZH, Zhang YP, Deng XB, Song QH, Liu WJ, Deng Y, Tang JW, Liao ZY, Zhao JF, Song L, Yang LY (2013) Interannual and seasonal variability of water use efficiency in a tropical rainforest: results from a 9year eddy flux time series. *J Geophys Res Atmos* 120:464–479
- Testi L, Orgaz F, Villalobos FJ (2006) Variations in bulk canopy conductance of an irrigated olive (*Olea europaea* L.) orchard. *Environ Exp Bot* 55(1):15–28
- Viswanadham Y, Sa LDDA (1987) Ratios of eddy transfer coefficients over the Amazon forest. *For Hydrol Watershed Manag* 167:1810–1814
- Wang D, Gartung J (2010) Infrared canopy temperature of early-ripening peach trees under postharvest deficit irrigation. *Agric Water Manag* 97:1787–1794
- Wang YP, Leuning R (1998) A two-leaf model for canopy conductance, photosynthesis and partitioning of available energy I: model description and comparison with a multi-layered model. *Agric For Meteorol* 91:89–111
- Zhang K (1966) An analysis on the characteristics and forming factors of climates in the southern part of Yunnan. *Acta Meteor Sin* 33:210–230
- Zhang JL, Zhu JJ, Cao KF (2007) Seasonal variation in photosynthesis in six woody species with different leaf phenology in a valley savanna in southwestern China. *Trees* 21:631–643
- Zhang B, Liu Y, Xu D, Cai J, Li F (2011) Evapotranspiration estimation based on scaling up from leaf stomatal conductance to canopy conductance. *Agric For Meteorol* 151(8):1086–1095
- Zhang YJ, Meinzer FC, Qi JH, Goldstein G, Cao KF (2013) Midday stomatal conductance is more related to stem rather than leaf water status in subtropical deciduous and evergreen broadleaf trees. *Plant Cell Environ* 36:149–158
- Zhang YJ, Holbrook NM, Cao KF (2014) Seasonal dynamics in photosynthesis of woody plants at the northern limit of Asian tropics: potential role of fog in maintaining tropical rainforests and agriculture in Southwest China. *Tree Physiol*
- Zhang X, Zhang Y, Sha L, Wu C, Tan Z, Song Q, Liu Y, Dong L (2015) Effects of continuous drought stress on soil respiration in a tropical rainforest in southwest China. *Plant Soil* 394:343–353